Surface plasmon resonance-based aptasensor for direct monitoring of thrombin in a minimally processed human blood

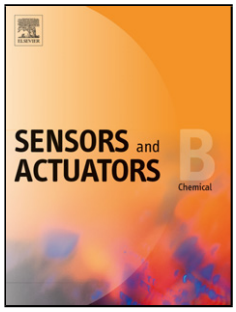

Surface plasmon resonance-based aptasensor for direct monitoring of thrombin in a minimally processed human blood

Daria Kotlarek, Federica Curti, Mariia Vorobii, Roberto Corradini (Supervision) (Funding acquisition), Maria Careri (Supervision) (Funding acquisition), Wolfgang Knoll (Supervision) (Funding acquisition), Cesar Rodriguez-Emmenegger (Supervision) (Funding acquisition), Jakub Dostálek (Supervision) (Funding acquisition)

PII: S0925-4005(20)30725-5

DOI: https://doi.org/10.1016/j.snb.2020.128380

Reference: SNB 128380

To appear in: *Sensors and Actuators: B. Chemical*

Received Date: 26 February 2020

Revised Date: 26 May 2020

Accepted Date: 27 May 2020

Please cite this article as: Kotlarek D, Curti F, Vorobii M, Corradini R, Careri M, Knoll W, Rodriguez-Emmenegger C, Dostálek J, Surface plasmon resonance-based aptasensor for direct monitoring of thrombin in a minimally processed human blood, *Sensors and Actuators: B. Chemical* (2020), doi: https://doi.org/10.1016/j.snb.2020.128380

Surface plasmon resonance-based aptasensor for direct monitoring of thrombin in a minimally processed human blood

Daria Kotlarek[a], Federica Curti[a,b], Mariia Vorobii[c], Roberto Corradini[b], Maria Careri[b], Wolfgang Knoll[a], Cesar Rodriguez-Emmenegger*[,c], Jakub Dostálek*[,a]

[a] Biosensor Technologies, AIT-Austrian Institute of Technology GmbH, Konrad-Lorenz-Straße 24, 3430 Tulln an der Donau, Austria

[b] Department of Chemistry, Life Sciences and Environmental Sustainability, University of Parma, Parco Area Delle Scienze, 17/A, 43124, Parma, Italy

[c] DWI − Leibniz Institute for Interactive Materials and Institute of Technical and Macromolecular Chemistry, RWTH Aachen University, Forckenbeckstraße 50, 52074 Aachen, Germany

Corresponding Authors

* Jakub Dostalek, PhD, E-mail: jakub.dostalek@ait.ac.at. Phone: +43 (0) 50550 4470, Fax: +43 (0) 50550 4450

* Cesar Rodriguez-Emmenegger, PhD, E-mail: rodriguez@dwi.rwth-aachen.de. Phone: +49 (0) 241 80-23362, Fax: +49 (0) 241 80-23301.

Graphical abstract

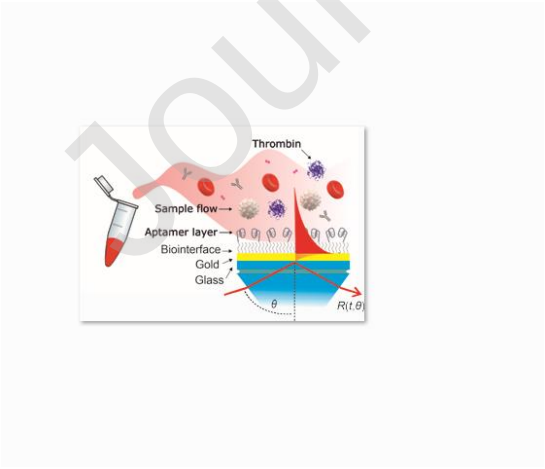

HIGHLIGHTS

- Antifouling polymer brushes with incorporated aptamer ligands specific to thrombin
- Affinity interaction analysis of three established aptamers on polymer brushes architecture compared to regular thiol SAM
- Superior antifouling properties of functionalized poly[(N-(2-hydroxypropyl)-methacrylamide)-*co*-(carboxybetaine methacrylamide)] brushes compared to regular thiol SAM allowed for direct label-free SPR detection of thrombin
- Implementation of direct detection of thrombin in 10% whole human blood at clinically relevant concentrations in 15 min

ABSTRACT

Optical affinity biosensors are pursued for timely monitoring of thrombin in human blood, which is of urgent need in tailored anticoagulation therapies. However, the unspecific deposition of molecules, cells, and aggregates from the blood at their surface (also termed fouling) severely hinders their development and impedes the deploying of this technology to everyday clinical practice. We addressed this challenge by designing surface plasmon resonance (SPR) sensor chip with an antifouling polymer brush architecture and incorporated thrombin aptamer bioreceptors. Poly[(*N*-(2-hydroxypropyl)-methacrylamide)-*co*-(carboxybetaine methacrylamide)] brushes were synthesized on gold sensor chip surface via photoinduced single-electron transfer living radical polymerization and postmodified with three thrombin aptamers (HD1 short, HD1 and HD22). The affinity interaction of the aptamer bioreceptors with thrombin (as well as with other molecules present in the blood) was investigated and changes in their performance when incorporated into the polymer brushes were characterized. The combination of brushes and aptamer bioreceptors allowed for the analysis of medically relevant concentrations of thrombin in the 10% blood by direct SPR detection format. This is the first time that the optical affinity biosensor is demonstrated for label-free analysis of biomarkers in a minimally processed human blood without a need for pre-separation steps. We believe that this system constitutes a basis for the future affinity biosensor applications that are suitable for the clinical settings and can be readily adapted to detect a range of important biological markers.

Keywords: surface plasmon resonance; polymer brushes; antifouling surface; aptamers; thrombin; whole human blood; point-of-care

1. Introduction

Thrombin is an essential enzyme of hemostasis and it keeps at check bleeding by initiating coagulation in healthy individuals. Its misbalance may lead to hemorrhage or thrombosis - severe conditions that are accompanied by excessive bleeding, pulmonary embolism, stroke, or myocardial infarction [1,2]. Therefore, the concentration of thrombin in the blood is an important marker in clinical practice. It dictates the anticoagulation strategy to be followed for patients subjected to cardiac surgery, extracorporeal membrane oxygenation therapy, and even dialysis. Notably, the lack of means to monitor changes in the concentration of this biomarker directly results in the administration of higher doses of anticoagulants. Although the anticoagulation may later be reversed (if some indirect test shows that the levels of thrombin are too low), this often causes a window of time in which the patient may suffer from hemorrhages. New biosensor technologies for rapid analysis of thrombin constitute a promising tool to prevent the hemostatic complications, tailor the anticoagulation therapy, and guide the timely decision making in the operating room. However, the unspecific interaction of blood-derived constituents with the surface of affinity biosensors (fouling) hinders the readout of the specific sensor signal and it is arguably the most limiting factor hampering their progress in the clinical applications [3].

The vast majority of reported label-free biosensor concepts with rapid direct detection format were demonstrated for the analysis of target analytes in buffer or diluted blood serum or plasma [4,5]. These results are only a pre-step towards the direct detection in minimally or unprocessed whole blood, which (arguably) represents the most challenging medium [6]. In order to overcome the problem of sensor fouling, there was implemented pre-separation of blood components by using a two-stage microfluidic platform [7], microfilter [8], continuous-flow diffusion filter [9] or by applying a centrifugal force [10]. In addition, there was pursued research on an alternative strategy to minimize the blocking of sensor surface with blood constituents based on coatings with antifouling properties including self-assembled monolayers (SAMs) with oligo(ethylene glycol) chains (OEG) [11,12], tethered zwitterionic groups [13] and grafting polymer chains forming brushes [14]. OEG-SAMs are formed by tightly packed ordered molecules that carry short OEG headgroups oriented towards the sample. The hydration of OEG moieties provides sufficient repellence from model matrices comprising proteins such as human serum albumin (HSA), fibrinogen, lysozyme, and immunoglobulin G (IgG) that are the most abundant constituents of blood. However, these SAMs fail to resist fouling when they are brought in contact with more complex biological media such as blood plasma and serum [15–17]. Improved resistance to fouling was achieved when the head-group of the SAM comprised zwitterionic groups. For instance, zwitterionic peptides were shown to prevent the unspecific protein adsorption from 2% serum [13] and 1% human whole blood [18]. Such advanced

performance is attributed to the ability of zwitterionic groups to structure water, which generates an enthalpic barrier to fouling. This barrier, however, cannot fully prevent adsorption of less diluted blood and undiluted blood plasma when introduced to SAM-based architectures. To date, further increased resistance to fouling has been achieved by several types of hydrophilic polymer brushes. This type of biointerface takes advantage of high-density polymer chains grafted to the sensor surface to prevent fouling by a combination of an enthalpic barrier, strong solvation, and an entropic penalty. The utilization of various hydrophilic polymer brushes has been reported, but among them, only several types fully prevented the fouling from undiluted blood plasma. Currently, the best antifouling performance has been achieved with zwitterionic carboxybetaines (methacrylate [19], acrylamide [20] and methacrylamide [CBMAA] [21]) and *N*-2-hydroxypropyl methacrylamide (HPMA) brushes [22].

Although the described biointerfaces were showed to repel blood plasma proteins, their properties often change when implemented to an affinity biosensor that requires their post-modification with bioreceptors. The chemical procedures employed in the ligation of the bioreceptor to the polymer brushes lead to irreversible changes in their structure and a concomitant loss of their antifouling performance [23]. To circumvent this problem, two antifouling monomers (CBMAA and HPMA) were statistically copolymerized in molar ratio 17:3 in order to provide only a small fraction of the side chains for the ligation of bioreceptors. This approach resulted in the minimal changes in the chemical structure of the polymer brushes and allowed preserving their antifouling properties. This concept was implemented in several surface plasmon resonance (SPR) – based sensors for the analysis of biological samples using the protein bioreceptors such as hepatitis B surface antigen-HBsAg or anti-fetuin-A IgY antibody [24–26].

In our recent work [27], we presented a compact SPR sensor device based on a gold-coated grating that was modified by poly(HPMA-*co*-CBMAA) brushes with HD1 aptamer and used for detection of thrombin in undiluted human plasma. In this approach, the optical probing is utilized through the analyzed sample, which is not suitable for the analysis of blood samples with large constituents that absorb and scatter light. Herein, we therefore further extended this work for the analysis of 10% human blood and investigate options to improve the performance of the sensor by using different thrombin DNA aptamer sequences that recognize two distinct binding sites of thrombin (exosite I and II). The DNA aptamers constitute an attractive alternative to the protein recognition elements as they can be engineered in a test tube and mass-produced by chemical synthesis [28]. In addition, aptamers exhibit better storage stability, and often their interaction with target molecules is reversible allowing for a facile regeneration of the sensor surface [29]. The HD1 short, HD1 and HD22 aptamers were incorporated in poly(HPMA-*co*-CBMAA) brushes on a surface of SPR sensor with Kretschmann configuration of attenuated total reflection method, where the optical probing is performed from the opposite side to the analyzed sample. There is demonstrated the importance of biointerface engineering and cross-reactivity of the used aptamers with abundant proteins present in the blood

(HSA, IgG, and prothrombin) in order to enable rapid analysis of minimally processed blood samples. Such biointerface was tailored for label-free and rapid detection of thrombin at clinically relevant concentrations in human blood samples diluted to 10%. According to our knowledge, this is the first label-free affinity biosensor that can be operated in such manner.

2. Materials and methods

2.1. Materials and reagents

Thrombin aptamers were custom synthesized by Integrated DNA Technologies (Belgium). There were used two variants of each aptamer, either with amine or with biotin terminal group (HD1 short: amino modifier C6 5'-TTT TTG GTT GG-3', M_W = 3.6 kDa; biotin 5'-TTT TTT TTT TGG TTG G-3', M_W = 5.3 kDa; HD1: amino modifier C6 5'-TTT TTG GTT GGT GTG GTT GG-3', M_W = 6.5 kDa; biotin 5'-TTT TTT TTT TGG TTG GTG TGG TTG G-3', M_W = 8.2 kDa; scrambled biotin 5'-TTT TTT TTT TGG TGG TGG TTG TGG T-3' M_W = 8.2 kDa; HD22: amino modifier C6 5'-TTT TTA GTC CGT GGT AGG GCA GGT TGG GGT GAC T-3', M_W = 10.9 kDa; biotin 5'-TTT TTT TTT TAG TCC GTG GTA GGG CAG GTT GGG GTG ACT-3', M_W = 12.5 kDa). Thrombin purified from human plasma (M_W = 37 kDa) was obtained from Enzo Life Sciences (Switzerland). Human prothrombin native protein (M_W = 72 kDa) and human immunoglobulin G (hIgG, M_W = 150 kDa) were purchased from Thermo Scientific (Germany). The single donor whole human blood was obtained from Innovative Research (USA). Biotinylated alkane OEG-thiol (thiol-OEG-biotin, SPT-0012D) and (11-mercaptoundecyl) triethyleneglycol (thiol-OEG-OH, SPT-0011) were purchased from SensoPath Technologies Inc. (USA). 1-Ethyl-3-(3-dimethylaminopropyl)-carbodiimide (EDC), *N*-hydroxysuccinimide (NHS) and neutravidin protein were purchased from Thermo Scientific (Austria). Acetic acid, sodium acetate, sodium chloride, HEPES, Tween 20, argatroban monohydrate (M_W = 526.65 g/mol), Human Serum Albumin (HSA, M_W = 6.6 kDa) and Hellmanex III were purchased from Sigma-Aldrich (Austria). Phosphate buffer saline tablets (PBS: 140 mM NaCl, 10 mM phosphate, 3 mM KCl, pH 7.4) came from Calbiochem (Germany). All buffer solutions were prepared by using ultrapure water (arium pro, Sartorius Stedim, Germany). PBS Tween (PBST) was prepared by adding Tween 20 (0.05%) to PBS solution. 10 mM sodium acetate buffer (SA, pH 5) was prepared from acetic acid and sodium acetate. The HEPES buffer was used with the pH adjusted by NaOH (pH 7.5). Extra dry dimethyl sulfoxide (DMSO, 99.7+%) was acquired from Acros Organic (Germany). Tris[2-(dimethylamino)ethyl]amine (Me_6TREN, 99+%) were obtained from Alfa Aesar (Germany). Copper (II) bromide ($CuBr_2$, 99.999% trace metal basis) was purchased from Sigma Aldrich (Germany). Initiator, ω-mercaptoundecyl bromoisobutyrate [30], and monomer, *N*-(2-hydroxypropyl) methacrylamide (HPMA) [31], were synthesized according to the procedures published before. Monomer, (3-methacryloylaminopropyl)-(2-carboxyethyl)-dimethylammonium (carboxybetaine methacrylamide, CBMAA), was synthesized using a modified version of the

procedure reported earlier [16], Ethanol (EtOH) came from VWR Chemicals (Germany). Milli-Q water was obtained using an Elga US filter Purelab Plus UF purification system (PL5113 02) (UK).

2.2. Preparation of SPR sensor chips

BK7 glass substrates (Carl Roth, Austria) and LASFN9 glass substrates (Hellma GmbH, Germany) were cleaned by subsequent sonication in a 1% aqueous solution of Hellmanex III, in ultrapure water and in ethanol. Then, chromium (2 nm thickness) and gold (50 nm thickness) layers were deposited on their top by vacuum thermal evaporation (HHV AUTO 306 from HHV LTD, UK) in vacuum better than 10^{-6} mBar. In addition, commercial SPR sensor chips already coated with thin gold film (XanTec bioanalytics GmbH, Germany) were used. For the experiments with thiol SAM biointerface, the BK7 glass and XanTec SPR sensor chips were overnight immersed in 1 mM ethanolic solution of thiol-OEG-biotin and thiol-OEG-OH (molar ratio 1:4) in order to form mixed SAM. The LASFN9 glass substrates coated with gold were used for the experiments with polymer brushes. The polymer brushes of poly(HPMA-*co*-CBMAA) were synthesized by photoinduced single-electron transfer living radical polymerization (SET-LRP). For the formation of SAM of initiator, gold-coated LASFN9 glass substrates were immersed overnight in 2.4 mM ethanolic solution of *ω*-mercaptoundecyl bromoisobutyrate. For the polymerization, 5.99 g (41.89 mmol) of HPMA and 1.79 g (7.39 mmol) of CBMAA were dissolved in 28 mL of dry DMSO. Simultaneously, a stock solution of the catalyst was prepared by dissolving 8.7 mg (39 μmol) of $CuBr_2$ and 62.5 μL (233.8 μmol) of Me_6TREN in 10 mL of dry DMSO. Both flasks were kept in the dark by wrapping them with aluminum foil. After the complete dissolution of all components, 1.2 mL of stock catalyst solution was mixed with dissolved monomers and degassed by bubbling N_2 for 1 h. Subsequently, polymerization solution was transferred to previously degassed (purging with N_2 for 30 min) vials containing gold-coated LASFN9 glass substrates with SAM of the initiator. The polymerization was conducted for 17 min by irradiating the vials inside a UV-reactor, consisting of a nail-curing device (four 9 W lamps, λ_{max} = 365 nm) kept at room temperature by fanning with a ventilator. After polymerization, the reaction was stopped by exposing a reaction mixture to air and adding DMSO. The samples were removed from the reactor and washed twice with EtOH and Milli-Q water and dried by blowing with N_2.

2.3. SPR biosensor instruments

Two SPR sensor instruments that rely on the Kretschmann configuration of the attenuated total reflection method with angular interrogation were used in the presented work. The affinity interaction analysis was performed by using a Reichert SR7000DC system with an integrated SR7120 autosampler instrument. XanTec sensor chips were used in this instrument and surface plasmons were resonantly excited at a wavelength of 780 nm. As this instrument was not suitable for the studies on

sensor chips with the polymer brushes (the increased refractive index of the brushes shifted the SPR angle θ out of the measurable range), additional in-house developed SPR spectrometer that utilizes same type angular spectroscopy of surface plasmons was employed. The SPR sensor chip carrying either the mixed thiol-OEG/biotin SAM or poly(HPMA-*co*-CBMAA) brushes was optically matched to the LASFN9 glass prism by using a refractive index matching oil (Cargille Inc., USA) and mounted on a rotation stage to control the angle of incidence θ. The beam from HeNe laser at a wavelength of 633 nm that was coupled to the 90° LASFN9 glass prism in order to resonantly excite surface plasmons (Figure 1a). The intensity of the reflected beam was measured as a function of angle of incidence $R(\theta)$ or time $R(t)$ at an angle θ that was fixed close to the SPR dip [on the resonance edge with the highest slope in $R(\theta)$]. The instrument was controlled by dedicated software (Wasplas, Max Planck Institute for Polymer Research, Mainz, Germany). A flow-cell with a 5 µL reaction chamber made from a thin PDMS gasket (thickness of 100 µm from Specialty Silicone Products, Inc., USA, cut by Institute of Photonics and Electronics, Czech Academy of Sciences) was clamped against the SPR chip surface. Analyzed liquid samples were flowed by using a Tygon tubing and a peristaltic pump (Ismatec, Germany) with a flow rate of 50 mL min^{-1}. In order to compare the SPR sensor signal from the two SPR instruments, the response R was converted to refractive index units (RIU) by a calibration step with the bulk refractive index changes upon the flow of aqueous solutions spiked with 1, 2 and 4 wt% of sucrose (inducing bulk refractive index increase of $\Delta n_s = 1.4 \times 10^{-3}$; 2.8×10^{-3}; 5.6×10^{-3} RIU, respectively).

2.4. Immobilization of the thrombin aptamer

The immobilization of thrombin aptamers was performed *in situ* on the SPR sensor chips that were previously modified with either mixed thiol-OEG/biotin SAM or poly(HPMA-*co*-CBMAA) brushes. The SPR sensor chip carrying the mixed thiol SAM was firstly rinsed with PBS (pH 7.4) for 5 min in order to establish a baseline in the SPR signal $R(t)$. Then 50 µg·mL^{-1} neutravidin dissolved in PBS was flowed over the surface for 90 min in order to conjugate to the biotin moieties tethered at the sensor surface. The excess of neutravidin was rinsed off by using PBS for 5 min and finally, 1 µM solution of biotinylated aptamer (HD1 short, HD1 or HD22) in PBS was reacted with the sensor surface for 15 min and then washed with PBS for 5 min. The immobilization of aptamers on the poly(HPMA-*co*-CBMAA) brushes was carried out by amine coupling. The baseline in the SPR signal $R(t)$ was established upon the 5 min flow of PBS (pH 7.4) that was then replaced with SA buffer for 5 min (pH 5.0). Subsequently, the carboxylic moieties of the betaine monomer in the poly(HPMA-*co*-CBMAA) brushes were activated by a freshly prepared aqueous solution of EDC (0.4 M) and NHS (0.1 M) for 10 min. The activated polymer film was shortly rinsed with SA (pH 5.0) and HEPES buffer (pH 7.5) and then 1 µM solution of aptamer (HD1 short, HD1 or HD22) with the amine terminal group was flowed over the surface for 30 min in order to form covalent bonds with the chains

of polymer brushes. Subsequently, the unbound aptamers were rinsed off with HEPES (pH 7.5) and the functionalized sensor surface was incubated in PBS for 90 min in order to let the unreacted active ester groups hydrolyze.

2.5. Assay for interaction analysis and detection in buffer and blood samples

The SPR sensor chips functionalized with aptamer bioreceptors were used for the affinity capture of thrombin from either PBS or whole human blood diluted to 10% with PBS. The same protocol was adopted for the interaction study of aptamers with other proteins that may interfere with the thrombin binding including HSA, IgG, and prothrombin. Since the addition of exogenous thrombin to the whole blood containing fibrinogen would trigger its coagulation, we supplemented the analyzed samples with the anticoagulant argatroban (38 μM concentration). Firstly, the baseline in the SPR sensor signal $R(t)$ was established upon the flow of PBS(T) for 5 min. Then, the analyzed sample spiked with investigated biomolecules was flowed over the surface and the reaction time was set to 30-60 min (in affinity interaction study) or to 15 min (in rapid detection experiment). The sensor surface was afterward rinsed with PBS(T) for 30 min (in affinity interaction study) or 5 min (in rapid detection experiment) and subsequently regenerated with an aqueous solution of 2 M NaCl for 2 min followed by the rinsing with PBS(T). The control experiment was performed analogously on the non-functionalized surface or on the surface with anchored aptamers exhibiting scrambled sequence.

2.6. Calculation of surface mass density

A model was established in order to determine surface mass density Γ of covalently immobilized aptamers and affinity captured thrombin from measured changes in SPR signal $R(t)$ acquired in RIU for sensor chips with mixed thiol-OEG/biotin SAM and polymer brushes architectures. The surface mass density was calculated by using the formula $\Gamma = (n_p - n_s) \cdot d_p / (\partial n / \partial c)$,[32] where n_p and n_s are the refractive indices of oligonucleotide/protein layer and an aqueous sample, respectively, and d_p corresponds to the thickness of the oligonucleotide/protein layer. The factor $\partial n / \partial c = 0.2$ mm^3 mg^{-1} relates the changes in refractive index and concentration of biomolecules bound to the surface [33]. As the probing surface plasmon field (that evanescently decay from the gold surface) responds differently to molecular binding occurring at a short distance of 3 nm (for thiol SAM) and long distance of 42 nm (for polymer brushes), the used respective converting factors $\Gamma/\delta R$ are different. Further, we used the factors of $\Gamma/\delta R$= 510 ng mm^{-2} RIU^{-1} for SAM and $\Gamma/\delta R$ = 450 ng mm^{-2} RIU^{-1} for polymer brushes interface. These factors where obtained for the probing SPR wavelength of 633 nm from Fresnel reflectivity-based simulations implemented in Winspall software (Max Planck Institute for Polymer Research, Germany) as described in the supporting information (SI).

2.7. Evaluation of SPR binding kinetics

The association binding rate k_{on} and dissociation binding rate k_{off} describing the interaction between thrombin in a liquid sample and aptamers immobilized on mixed thiol-OEG/biotin SAM were obtained by the analysis of measured SPR sensorgrams. Thrombin was dissolved in PBS at a concentration of c = 5, 10, 15, 20, 35, 50, 100 and 500 nM and these samples were sequentially flowed over the sensor surface that was functionalized with HD1 short (60 min reaction time), HD1 (30 min reaction time), and HD22 (30 min reaction time) in order to affinity bind and followed by 30 min rinsing with the PBS to dissociate from the surface. In between the analysis of samples with different thrombin concentrations, the sensor chip was regenerated with 2 M NaCl. The sensorgrams $R(t)$ acquired by using the XanTec SPR chip and Reichert SPR instrument were fitted with a 1:1 binding model that was implemented in Prism 8 (GraphPad Software) and by a model taking into account diffusion-limited kinetics in Scrubber 2 (BioLogic Software). For details of the fitting model, the reader is referred to the SI.

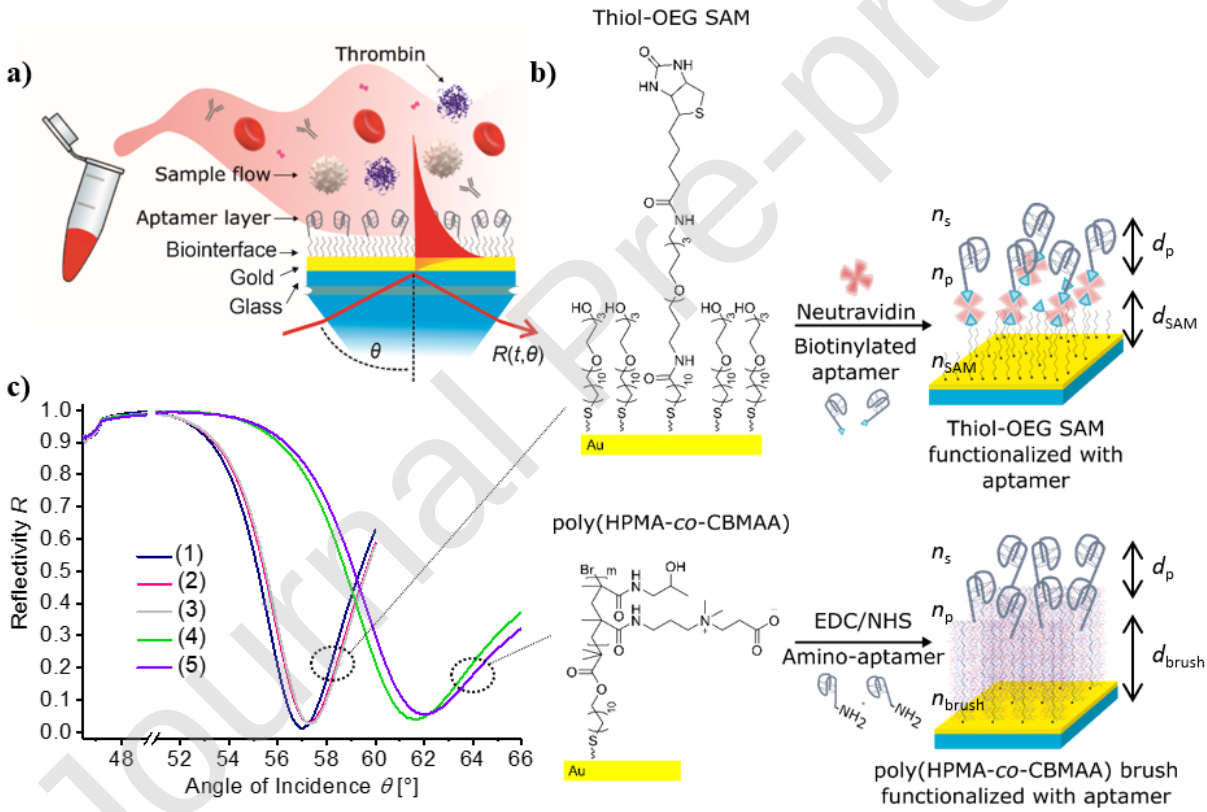

Figure 1. a) The schematic of the SPR sensor chip that is modified with b) thiol-OEG SAM or poly(HPMA-*co*-CBMAA) architecture in order to couple thrombin aptamer at its surface. c) Angular reflectivity SPR spectra acquired at the wavelength of 633 nm on SPR sensor chip carrying (1) thiol-OEG SAM, (2) thiol-OEG SAM with neutravidin, (3) thiol-OEG SAM with neutravidin and immobilized aptamer HD22 compared to that measured on (4) pristine polymer brushes and (5) polymer brushes functionalized with aptamer HD22.

3. Results and discussion

3.1. Immobilization of thrombin aptamers

In order to enable direct detection of thrombin in minimally processed whole blood, there was pursued a biointerface architecture based on poly(HPMA-*co*-CBMAA) brushes that specifically bind target thrombin analyte from the analyzed sample at the sensor surface by the use of aptamer bioreceptors, see Figure 1a. In order to benchmark the performance of this biointerface, additional regular mixed thiol SAM modification with OEG-OH and OEG-biotin headgroups [32] was used. As Figure 1b illustrates, we investigated these sensing surfaces in conjunction with three thrombin aptamer bioreceptors – HD1 short, HD1 and HD22 – that were anchored at the sensor surface by using amine coupling on poly(HPMA-*co*-CBMAA) brushes via a biotin tag for mixed thiol-OEG/biotin SAM interface.

The immobilization procedure was monitored by SPR and both reflectivity curves $R(\theta)$ before and after the bioreceptor immobilization and the SPR signal kinetics $R(t)$ upon the surface reaction were acquired. The example presented in Figure 1c shows that resonant excitation of surface plasmons on mixed thiol-OEG/biotin SAM surface with incorporated biotin moieties manifests itself as a dip in $R(\theta)$ centered at an angle of incidence of $\theta = 57.00°$ (1). The SPR angle changes to $\theta = 57.28°$ (2) after the conjugation of neutravidin with the biotin headgroups on thiol SAM and it further shifts to $\theta = 57.33°$ when the immobilization of the biotinylated aptamer HD22 is carried out (3). For the SPR chip carrying the pristine poly(HPMA-*co*-CBMAA) brushes, the SPR occurs at a higher angle of $\theta = 61.60°$ (4) because of the increased thickness of the polymer brush layer (d_{brush}~42.0 nm measured by ellipsometry, SI, Figure S1) in comparison to the SAM architecture (~ 3.0 nm, SensoPath manufacturer catalog). The covalent coupling of the amine-terminated aptamer HD22 to carboxylic groups present at the chains of polymer brushes leads to the additional shift of SPR angle to $\theta = 62.00°$ (5).

SPR sensor kinetics $R(t)$ were recorded upon the immobilization of aptamer bioreceptors on the poly(HPMA-*co*-CBMAA) brushes and mixed thiol-OEG/biotin SAM. The sensor response ΔR in RIU was acquired for all three aptamers from the respective kinetics of SPR sensor signal $R(t)$ and it was subsequently converted to changes in surface mass density Γ and surface density (by dividing these values with a respective molecular weight of biomolecules - *MW*) as can be seen in the overview presented in Table 1. The SPR sensor response of $\Delta R = 137$, $\Delta R = 317$, $\Delta R = 549$ μRIU was measured for the coupling of HD1 short, HD1 and HD22 aptamers, respectively, on the mixed thiol-OEG/biotin SAM architecture. These data were obtained from the kinetics presented in Figure S3a and they stand in a good agreement with the previously reported values [34,35]. The SPR sensor response was 8 - 11 times higher on the poly(HPMA-*co*-CBMAA) brushes yielding $\Delta R = 1536$, $\Delta R = 2409$ and

ΔR = 4361 μRIU for HD1 short, HD1, and HD22 aptamers, respectively, as determined from data in Figure S3b. These results translate to a surface density of Γ/MW=0.013 pmol mm^{-2}, 0.020 pmol mm^{-2} and 0.022 pmol mm^{-2} for HD1 short, HD1 and HD22 respectively, on the mixed thiol-OEG/biotin SAM surface. Interestingly, the density ratio of the aptamer to the tetrafunctional neutravidin (which served as a linker between the biotin groups in the SAM and aptamer biotin terminal group) was in all cases close to one. This confirms that the density of these bioreceptors was controlled by the density of immobilized neutravidin linker (Γ = 0.019 pmol mm^{-2} determined from measured SPR sensor response of ΔR = 2289 μRIU).

The immobilization of aptamers on poly(HPMA-*co*-CBMAA) brush biointerface allowed reaching a substantially higher surface density of Γ/MW=0.194 pmol mm^{-2}, 0.168 pmol mm^{-2} and 0.182 pmol mm^{-2} for HD1 short, HD1 and HD22 respectively. This is the result of the organization of chains in the brushes at the interface which is less rigid than in SAMs allowing accessing not only to the last monomer units but to others in the last thermal blob. Furthermore, while in SAMs the immobilization of the aptamer required a very bulky neutravidin, in brushes the immobilization was direct which enhances further the binding sites available. Importantly, the chemical design of the selected brushes can provide efficient means to compensate for the negative charge introduced by the aptamer immobilization (which often leads to undesired unspecific interactions). The balance between the carboxylate groups and the quaternary ammonium from the betaine monomer guarantees the initial neutral zeta potential of the polymer brush structure. Upon the activation, with the carbodiimide crosslinking agent the carboxylate groups are turned to the active esters that lead to establishing of weakly positive zeta potential. This results in the electrostatic attraction of the negatively charged aptamer molecules that is reflected in the rapid kinetics within the first 3 min of the reaction (see Figure S3b). The gradual incorporation of the aptamers introduces to the polymer brushes negative charge that slows down the reaction by Coulombic interaction. Moreover, the slower part of the reaction kinetics occurring after 3 min can be attributed to the immobilization of the aptamers deeper in the poly(HPMA-*co*-CBMAA) brush structure, which is affected by the hindered molecular diffusion in the crowded polymer brushes structure.

Table 1. Comparison of the surface mass density (middle columns) and respective surface density Γ/MW (right columns) of immobilized aptamers on thiol-OEG SAM and polymer brushes (upper part) and surface density of thrombin that is affinity captured in saturation at these biointerfaces (bottom part).

	Thiol-PEG SAM	**Polymer brushes**	**Thiol-PEG SAM**	**Polymer brushes**	**Thiol-PEG SAM**	**Polymer brushes**

Aptamer	µRIU		pg/mm²		pmol/mm²	
HD 1 short	137 ± 19	1536 ± 240	70 ± 10	691 ± 108	0.013 ± 0.002	0.194 ± 0.030
HD1	317 ± 23	2409 ± 603	162 ± 12	1083 ± 271	0.020 ± 0.001	0.168 ± 0.042
HD22	549 ± 19	4361 ± 750	280 ± 10	1960 ± 337	0.022 ± 0.001	0.182 ± 0.031
Thrombin	**µRIU**		**pg/mm²**		**pmol/mm²**	
HD 1 short	208 ± 3	-	106 ± 2	-	0.003 ± 0.001	-
HD1	510 ± 74	1393 ± 44	260 ± 38	626 ± 20	0.007 ± 0.001	0.017 ± 0.001
HD22	374 ± 25	662 ± 329	191 ±13	298 ± 148	0.005 ± 0.001	0.008 ± 0.004

3.2.Thrombin-aptamer affinity interaction analysis

The characteristics of affinity interaction between thrombin and the aptamers HD1 short, HD1, and H22 were determined by the use of SPR for mixed thiol-OEG/biotin SAM. For this purpose, PBS was spiked with a concentration of thrombin of c=5, 10, 15, 20, 35, 50, 100 and 500 nM and flowed sequentially over the sensor surface with a regeneration step applied between each cycle. The measured SPR signal $R(t)$ for the association and dissociation phases was fitted with a kinetic model as can be seen in Figure 2. This model assumed the 1:1 interaction between the analyte and the ligand and simultaneous fitting of measured curves for all concentrations was performed using non-linear regression. For the truncated version of HD1 aptamer (HD1 short), the obtained association rate of $k_{on} = 1.7 \cdot 10^6\,M^{-1}s^{-1}$ and dissociation rate $k_{off} = 21 \cdot 10^{-3}\,s^{-1}$ (according to our knowledge measured for the first time) yields an equilibrium dissociation constant of K_d = 12 nM. The interaction of longer HD1 and HD22 aptamers exhibited higher affinity and therefore an additional mass transfer coefficient k_m had to be introduced to the fitting. However, the association and dissociation binding rates for HD1 and HD22 aptamers were not possible to accurately determine from the acquired data, and only equilibrium dissociation constant of K_d <5 nM could be estimated (see the summary in Figure 2a). In comparison with literature, the herein reported values of equilibrium dissociation constant K_d are in the lower range of reported values. It is worth noting these values vary over a wide range from 1.19 nM [36] to 171 nM [37] for HD1 aptamer and from 2.4 nM [38] to 110 nM [37] for HD22.

a)

K_d [nM]	Thrombin	Prothrombin
HD 1 short	12	-
HD1	<5	39±9
HD22	<5	>1000

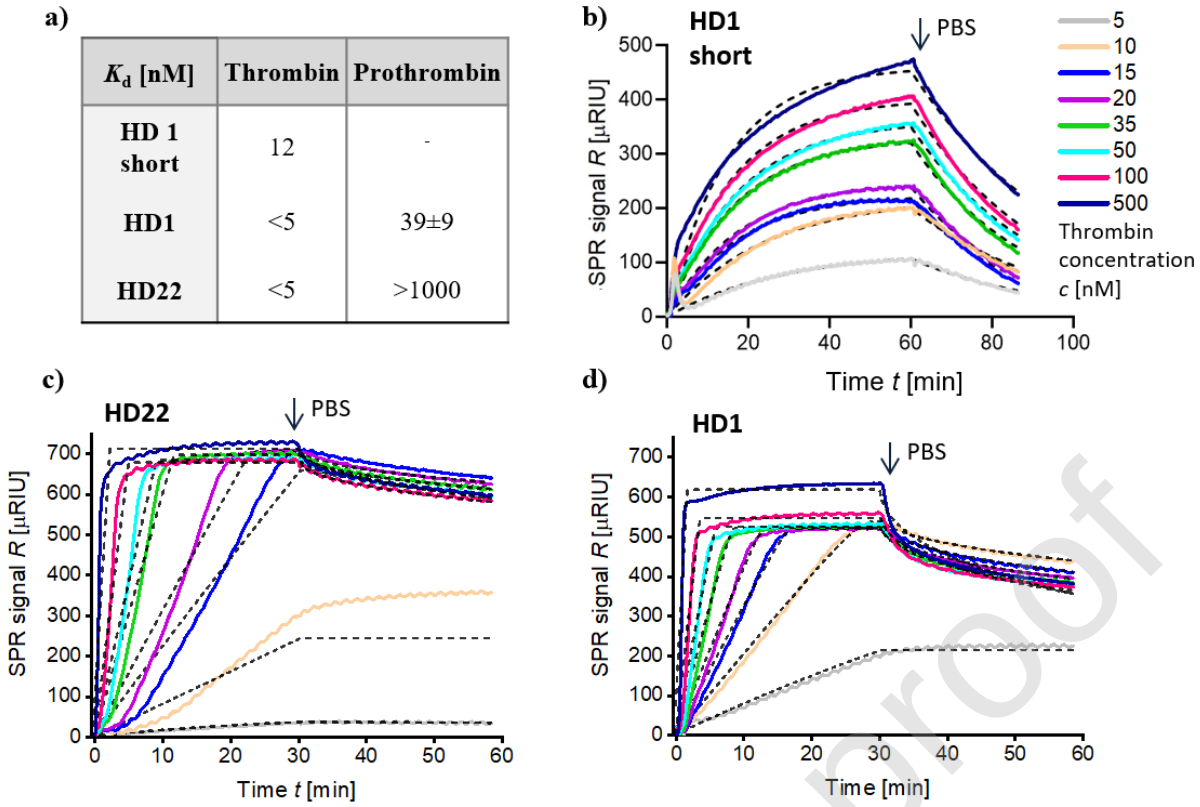

Figure 2. Global analysis measurement affinity binding rates of thrombin with three aptamer ligands. a) The table summarizes the determined equilibrium dissociation affinity constants and the graphs show the SPR sensorgrams for the interaction of analyte concentration *c*=5; 10; 15; 20; 35; 50; 100 and 500 nM on the sensor surface with thiol-OEG SAM functionalized with b) HD1 short, c) HD22 and d) HD1 aptamers. The solid lines present experimental data and dashed lines show the fitted curves. The arrows indicate the end of the association phase and the beginning of the dissociation phase.

3.3 Specificity of thrombin-aptamer affinity interaction

In order to verify the specificity of the used aptamers HD1 and HD22, their interaction with abundant biomolecules that constitutes human blood was observed with in-house developed SPR biosensor instrument. These include human serum albumin (HSA), human immunoglobulin G (hIgG), and prothrombin. In the blood of healthy donors, HSA is present at about 500 µM concentration, hIgG at 80 µM and prothrombin at 1.4 µM [39]. It is worth noting that prothrombin is structurally related to thrombin and HD1 aptamer recognizes the thrombin exosite I and II, while HD22 aptamer affinity binds solely to exosite II [36]. SPR affinity interaction study showed that HD1 also binds to prothrombin with the equilibrium dissociation constant of K_d=37 nM, while HD22 did not interact

with this prothrombin (aptamers were attached via biotin tag to dextran polymer chains anchored to the gold surface) [36].

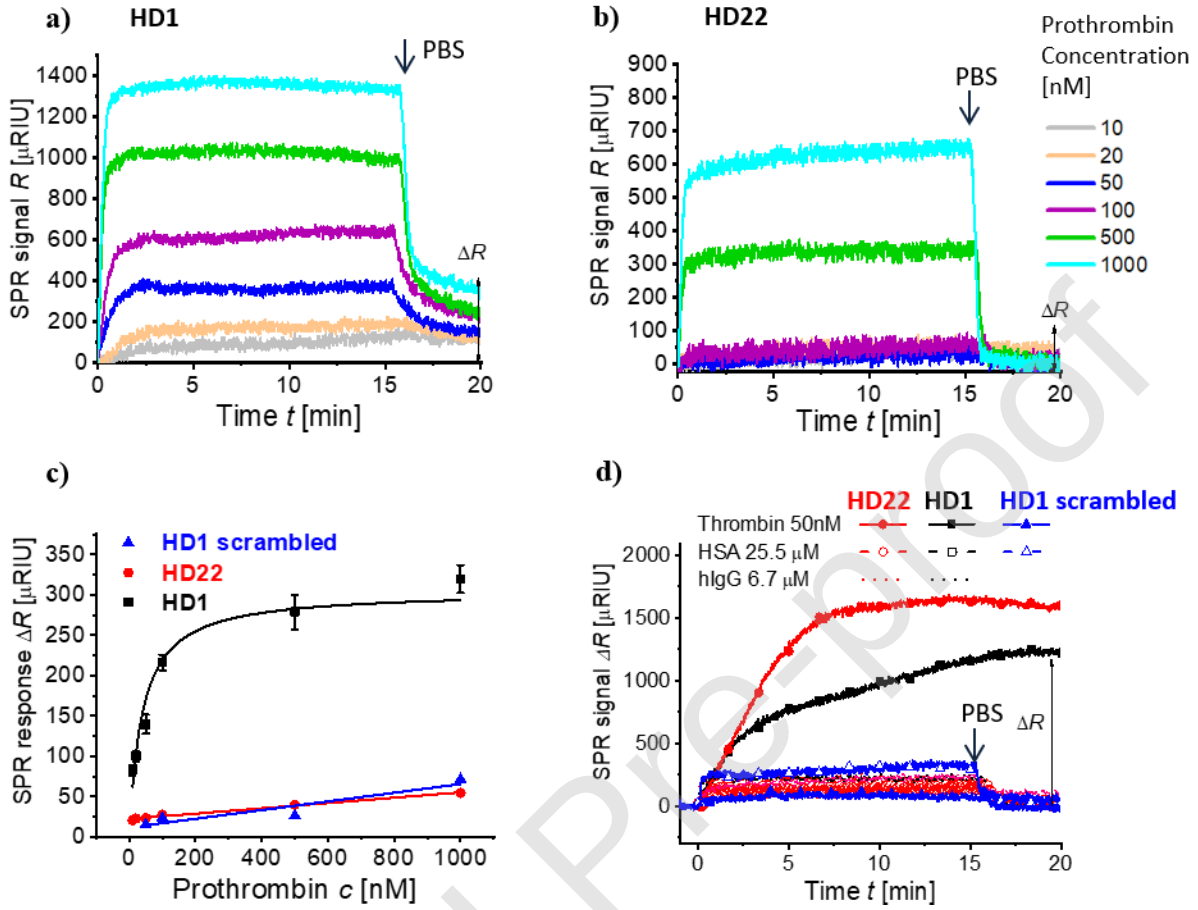

Figure.3 Specificity binding measurements of prothrombin, HSA and hIgG. The graphs show the SPR sensorgrams for the interaction with prothrombin at a concentration of c=10, 20, 50, 100, 500 and 1000 nM on the sensor surface with thiol-OEG SAM functionalized with a) HD1 and b) HD22 aptamers. c) The respective calibration curves are established. d) The interaction of HSA at 25.5 μM and hIgG at c=6.7 μM.

Further, we investigated potential interference to the thrombin direct assay due to the interaction of HD1 and HD22 aptamers with HSA, hIgG, and prothrombin by using a thiol-OEG-OH/biotin SAM. The SPR kinetics data presented in Fig. 3a and Fig. 3b reveal pronounced binding of prothrombin to HD1 aptamer at concentrations below 100 nM, while the interaction for HD22 aptamer was not measurable for concentrations up to 1 μM. The SPR signal change ΔR measured after 5 min rinsing of the surface that was exposed to prothrombin samples are plotted in Fig.3c. For the aptamer HD1, the plot is fitted with the Langmuir isotherm curve (as the association phase reached equilibrium) and the affinity dissociation constant of K_d = 39 ± 9 nM was determined. The dependence of ΔR on the surface

of HD22 aptamer could be fitted with linear function and indicates that the respective K_d is above the used concentration rate. Moreover, a similar trend was observed for scrambled HD1 aptamer sequence, which suggests that the small response may originate from unspecific sorption to the used thiol-OEG-OH/biotin SAM. In Fig.3d, there can be found the interaction of HD1 and HD22 with HSA and hIgG compared to that with thrombin. These findings show a negligible response for HSA at a concentration of 25.5 μM and hIgG at 6.7 μM. For the HSA, the same experiment was performed on the surface with a scrambled sequence of HD1 aptamer and a similar response suggests that the measured negligible change in SPR signal is attributed to unspecific sorption to the used thiol SAM-based biointerface.

3.4. Rapid detection of thrombin in buffer and blood samples

Sensor chips with poly(HPMA-*co*-CBMAA) brushes and mixed thiol-OEG/biotin SAM surface architectures were postmodified with the aptamers and their ability to specifically capture thrombin from 10% diluted whole blood and resist fouling was evaluated with direct SPR detection format. As can be seen in the acquired SPR kinetics data presented in Figure 4, the injection of 10% blood sample (with the endogenous thrombin present below pM concentration for healthy donors [40] into the sensor is accompanied by a rapid increase in the SPR signal $R(t)$ on both types of surfaces, which can be attributed to a change in bulk refractive index n_s. On the surface with the polymer brushes, this SPR signal change is less pronounced as the surface plasmon evanescent field exponentially decays with the distance from the gold surface. Compared to a thinner layer of mixed thiol SAM of 3 nm (according to the provider of thiol-OEG-biotin), the hydrated brushes occupy up to 42 nm (as measured with ellipsometry, see Figure S1) to which the penetration of blood constituents is hindered. After 2.5 min, a slower gradual increase in the SPR signal $R(t)$ occurs due to the sorption of blood compounds to the surface. The 10% blood was flowed over the surface for 15 min and then the sensor surface was rinsed with PBS and the SPR signal $R(t)$ rapidly drops as the bulk refractive index n_s decreases. After an additional 5 min rinsing the SPR signal levels at a value that is higher than the original baseline by ΔR_0 = 1.60 and 2.1 mRIU on the brushes and 1.85 and 2.7 mRIU on the thiol-OEG SAM carrying HD22 and HD1 aptamers, respectively. This change is attributed to the unspecifically adsorbed molecules and cross-reaction of aptamers with abundant constituents in blood. The more pronounced response to this blank sample for the HD1-modified biointerface compared to that carrying HD22 aptamer can be attributed to HD1 affinity to prothrombin that is present in blood. Importantly, these molecules can be fully removed from the surface of the poly(HPMA-*co*-CBMAA) brushes by the regeneration step while on the mixed thiol-OEG/biotin SAM only 80% of the adsorbed mass density Γ was released. This observation can be explained by electrostatic interaction of blood components with negatively charged aptamers and affinity binding of prothrombin being the main origin of the binding on the surface of polymer brushes. Both these interactions can be disrupted by using a high concentration of Na^+ ions that shield the negative charge of the aptamers [41]. In the case

of functionalized mixed thiol-OEG/biotin SAM, there is a coexisting effect of irreversible protein adsorption (fouling) that cannot be prevented in the performed experiments.

In the subsequent second detection cycle, a 10% diluted blood sample was spiked with thrombin at a concentration of 20 nM and allowed to interact with the investigated biointerface architectures by using the same protocol. Measured SPR signal kinetics presented in Figure 4 shows that the slope of the gradual increase of the SPR signal $R(t)$ is substantially steeper on the poly(HPMA-*co*-CBMAA) brushes and it levels at a higher value of ΔR = 2.3 and 3.8 mRIU after the rinsing of the surface with immobilized aptamer HD22 and HD1, respectively. Importantly, on the thiol-OEG SAM, the SPR signal change does not substantially differ from that measured for a blank sample proving that this interface becomes blocked by the blood constituents and that it cannot be used for direct SPR analysis of such complex biofluid. Interestingly, HD1 short aptamer lost the ability to affinity capture the thrombin analyte after its incorporation to the poly(HPMA-*co*-CBMAA) brushes (data not shown) and thus it was not used in further experiments.

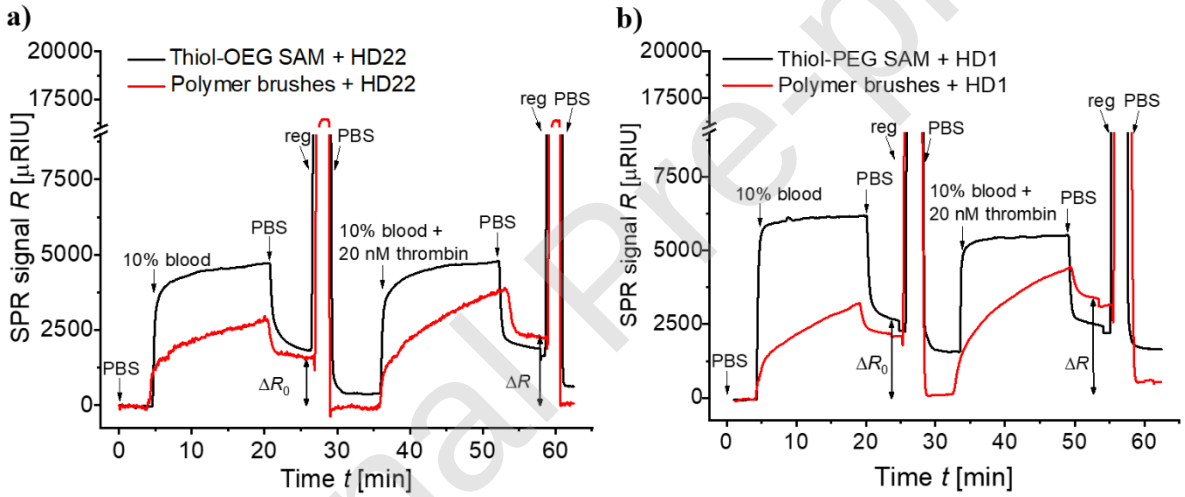

Figure 4. SPR sensor signal showing the interaction kinetics of blood compounds and thrombin in 10 % diluted whole blood on the sensor chip carrying thiol-OEG-SAM (black) or polymer brushes (red) functionalized with a) HD22 and b) HD1 thrombin aptamer.

Based on these observations, the functionalized poly(HPMA-*co*-CBMAA) brushes and HD1 and HD22 aptamers were employed for establishing a biosensor for the rapid direct detection of thrombin in 10% human blood samples. This biosensor was calibrated by using the developed protocol and 10% human blood samples containing c = 0, 5, 10, 15, 20 nM thrombin were sequentially injected with a regeneration step between detection cycles, see Figure 5a. The sensor response ΔR was determined as a difference in the SPR signal $R(t)$ before and after the flow of the analyzed liquid sample that was allowed to interact with the immobilized aptamer at the sensor surface for 15 min. The change in the

SPR signal ΔR was acquired after 5 min of rinsing with PBS. ΔR was plotted versus thrombin concentration c and fitted with a function $\Delta R = \Delta R_0 + \Delta R_{max} \cdot c / K_d / (1 + c / K_d)$, where ΔR_0 states for the change after the flow of a blank sample, ΔR_{max} is the response in saturation, and the parameter K_d corresponds to the equilibrium dissociation affinity constant. The error bar was determined as a standard deviation of at least three independent measurements. The SPR response ΔR of each sample was compensated with respect to the blank sample ΔR_0 and plotted against the analyzed concentration c in order to establish the calibration curves. The obtained data are presented in Figure 5b for the immobilized aptamers HD1 and HD22 and calibration curves measured for 10% blood samples are compared to those obtained with model samples when PBS was spiked with the target thrombin analyte.

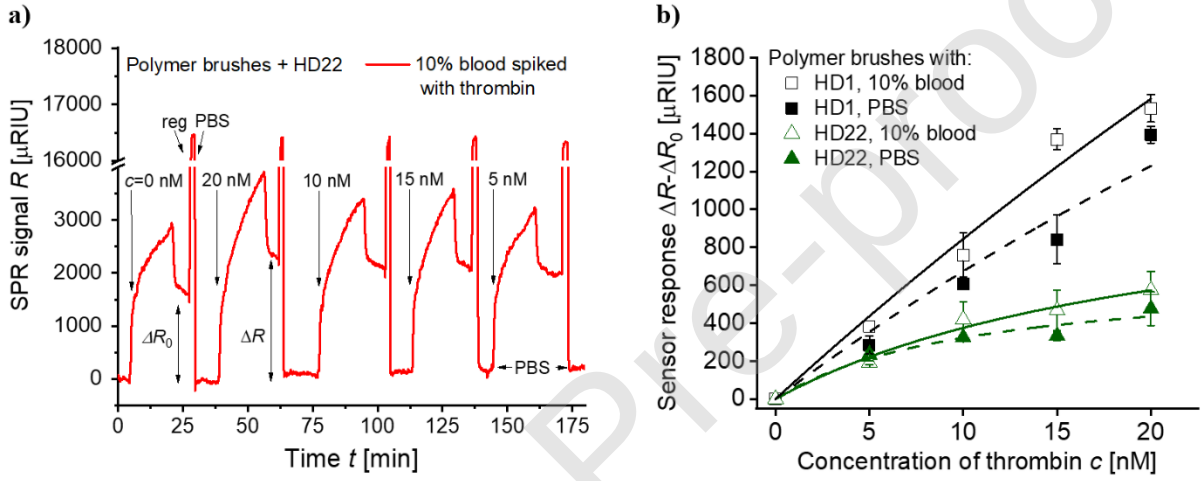

Figure 5. a) SPR sensor signal showing the kinetics of the affinity binding of thrombin from 10% diluted whole blood at a concentration of c=0, 5, 10, 15 and 20 nM on the sensor chip carrying polymer brushes functionalized with thrombin aptamer HD22. b) The calibration curves for detection of thrombin in PBS and 10% diluted whole blood established for polymer brushes functionalized with HD1 and HD22 aptamers.

Interestingly, the response of the SPR sensor to the presence of thrombin in 10% blood is higher than that for thrombin dissolved in PBS. The SPR response ΔR-ΔR_0 is increased by about 10% for HD22-functionalized polymer brushes and by 20% for the polymer brushes with the attached HD1 aptamer. The reason for this observation can be attributed to the potential activation of prothrombin by the captured thrombin (despite the used anticoagulant argatroban that prevents the coagulation in the bulk solution). This effect is less pronounced for HD22 aptamer as it does not exhibit affinity to prothrombin and it captures only thrombin by its exosite II with $K_d < 5$ nM. Contrary to HD22, the aptamer HD1 interacts with thrombin exosite I with $K_d < 5$ nM and also binds prothrombin with $K_d =$

39 nM. However, these interaction characteristics (measured with biotin-tagged aptamers in mixed thiol SAM surface) are probably substantially changed when aptamer bioreceptors are immobilized on poly(HPMA-*co*-CBMAA) brushes. The fitting of the obtained calibration curves with the Langmuir isotherm function yielded much higher effective values of K_d = 140.0 ± 6.5 and 23 ± 10 nM for HD1 and HD22 aptamer, respectively, for both PBS and 10% blood. This discrepancy can be partially attributed to the fact the used reaction time of 15 min did not allow for reaching equilibrium in the surface reaction (particularly for low thrombin concentrations *c*), which may be in addition slowed down by diffusion of the target analyte through the brushes polymer chains carrying higher density of aptamer ligands than the thiol SAM-based architecture (see Table 1). Moreover, the affinity interaction of aptamers is expected to be very sensitive to its local environment as it is reflected in the large variety of K_d values reported in the literature [36–38]. The presence of densely packed polymer chains constituting the brushes likely impacts the secondary structure of the aptamers necessary for the affinity interaction or leads to the steric hindrances and impeded access of thrombin molecules to the aptamer binding sites.

The limit of detection (LOD) was determined as a concentration where the fitted calibration curve intersects with the three times the standard deviation of the SPR sensor signal $\sigma(R[t])$. The used sensor instrument allowed for the measurement of bulk refractive index changes with the standard deviation of $\sigma=2\times10^{-5}$ RIU on the surface with poly(HPMA-*co*-CBMAA) brushes. It translates to LOD = 0.7 and 0.9 nM for HD1 aptamer-based sensor operated for detection of thrombin in 10% blood and PBS, respectively. For the HD22 aptamer, the achieved LOD was higher and reached 1 and 1.2 nM for 10% blood and PBS. The limit of detection in complex 10% blood is better than in PBS for both biointerfaces and it can be potentially explained by the cross-reaction with prothrombin and its interaction with a high surface concentration of affinity captured thrombin. In addition, let us note the previous work showed that HD1 aptamer (immobilized via biotin tag to the streptavidin-modified open dextran-based binding matrix) cannot be used for detection of thrombin in diluted blood plasma due to its cross-reaction with other biomolecules [36]. Contrary to this work, the herein presented results indicate that when incorporated to poly(HPMA-*co*-CBMAA) polymer brushes both aptamers HD1 and HD22 can serve for specific direct detection of thrombin in minimally processed 10% blood.

Giving the fact that the coagulation process occurs when the level of thrombin in the blood exceeds 5 – 20 nM [42], the obtained LOD = 0.7 nM for the direct rapid assay with HD1 aptamer in ten times diluted whole blood is in the lower part of this concentration range that indicates the risk of thrombosis. It is worth noting that the reported experiments focused on the investigation of the new antifouling biointerface by using a versatile home-built SPR instrument with limited accuracy (refractive index resolution of $\sigma=1.4\times10^{-5}$ RIU when operated with thiol SAM). In order to improve the LOD, another commercially available SPR sensor instruments with refractive index resolution at

10^{-7} level [43] are available and potentially applicable with the reported sensor chip biointerface architecture.

4. Conclusions

Thrombin aptamer bioreceptors HD1 and HD22 were successfully immobilized on poly(HPMA-*co*-CBMAA) brushes and utilized for the detection of thrombin in 10% whole human blood. The affinity interaction parameters of the aptamers on the novel polymer brush architecture were compared with a standard modification based on mixed thiol-OEG-OH/biotin SAM that was functionalized with the same aptamer sequences. The poly(HPMA-*co*-CBMAA) brushes allowed for the immobilizing of higher density of the aptamers at the surface and provided antifouling properties enabling repeating direct detection of thrombin in 10% whole blood by using regeneration in between the analysis cycles. Moreover, the limit of detection achieved for polymer brush architecture with HD1 aptamer is sufficient for the prediction of a thrombotic event and diagnosis of thrombosis. We believe that this work opens doors to the development of new diagnostic tools for rapid and direct detection of biomarkers in the minimally processed blood leading to guided therapeutic decision making and personalized treatment.

Supporting Information

The Supporting Information contains ellipsometry measurements of refractive index and thickness of polymer brush, characteristic of the SPR sensor, fitting parameters, and sensorgrams of aptamer immobilization and detection of thrombin in 10% human blood.

Declaration of interests

The authors declare that they have no known competing financial interests or personal relationships that could have appeared to influence the work reported in this paper.

Author Contributions

All authors have given approval to the final version of the manuscript.

Daria Kotlarek carrying out the experiments, evaluated results, manuscript writing.

Federica Curti carrying out the experiments, evaluated results, manuscript writing.

Mariia Vorobii carrying out the experiments, evaluated results, manuscript writing.

Roberto Corradini supervision, funding acquisition.

Maria Careri supervision, funding acquisition.

Wolfgang Knoll supervision, funding acquisition.

Cesar Rodriguez-Emmenegger supervision, funding acquisition, manuscript writing.

Jakub Dostalek supervision, funding acquisition, manuscript writing.

Acknowledgment

D.K. received funding from the European Union's Horizon 2020 research and innovation programme under grant agreement No 642787, Marie Sklodowska-Curie Innovative Training Network BIOGEL. J.D. was supported by Lower Austria project IKTHEUAP number WST3-F-5030820/010-2019. CR-E and M.V. acknowledge the support of the Deutsche Forschungsgemeinschaft (DFG) in the framework of the priority programme 2014 "Towards an Implantable Lung", project numbers: 346972946. Authors would like to thank Dr. Wojciech Ogieglo for conducting the ellipsometry measurements.

References

[1] B. Siegerink, A. Maino, A. Algra, F.R. Rosendaal, Hypercoagulability and the risk of myocardial infarction and ischemic stroke in young women, J. Thromb. Haemost. 13 (2015) 1568–1575. https://doi.org/10.1111/jth.13045.

[2] D.A. Wilkinson, A.S. Pandey, B.G. Thompson, R.F. Keep, Y. Hua, G. Xi, Injury mechanisms in acute intracerebral hemorrhage, Neuropharmacology. (2018) 240–248. https://doi.org/10.1016/j.neuropharm.2017.09.033.

[3] C. Blaszykowski, S. Sheikh, M. Thompson, Surface chemistry to minimize fouling from blood-based fluids, Chem. Soc. Rev. 41 (2012) 5599–5612. https://doi.org/10.1039/c2cs35170f.

[4] O. Tokel, F. Inci, U. Demirci, Advances in plasmonic technologies for point of care applications, Chem. Rev. 114 (2014) 5728–5752. https://doi.org/10.1021/cr4000623.

[5] S. Sang, Y. Wang, Q. Feng, Y. Wei, J. Ji, W. Zhang, Progress of new label-free techniques for biosensors: A review, Crit. Rev. Biotechnol. 36 (2016) 465–481. https://doi.org/10.3109/07388551.2014.991270.

[6] C. Rodriguez-Emmenegger, M. Houska, A.B. Alles, E. Brynda, Surfaces resistant to fouling from biological fluids: towards bioactive surfaces for real applications, Macromol. Biosci. 12

(2012) 1413–1422. https://doi.org/10.1002/mabi.201200171.

[7] E. Stern, A. Vacic, N.K. Rajan, J.M. Criscione, J. Park, R. Bojan, D.J. Mooney, M.A. Reed, T.M. Fahmy, Label-free biomarker detection from whole blood, Nat Nanotechnol. 5 (2010) 1–11. https://doi.org/10.1038/nnano.2009.353.Label-free.

[8] H.K. Chang, F.N. Ishikawa, R. Zhang, R. Datar, R.J. Cote, M.E. Thompson, C. Zhou, Rapid, label-free, electrical whole blood bioassay based on nanobiosensor systems, ACS Nano. 5 (2011) 9883–9891. https://doi.org/10.1021/nn2035796.

[9] B.S. Ferguson, D.A. Hoggarth, D. Maliniak, K. Ploense, R.J. White, N. Woodward, K. Hsieh, A.J. Bonham, M. Eisenstein, T. Kippin, K.W. Plaxco, H.T. Soh, Real-time, aptamer-based tracking of circulating therapeutic agents in living animals, Sci. Transl. Med. 5 (2013) 213ra165. https://doi.org/10.1371/journal.pone.0178059.

[10] C.E. Nwankire, A. Venkatanarayanan, T. Glennon, T.E. Keyes, R.J. Forster, J. Ducrée, Label-free impedance detection of cancer cells from whole blood on an integrated centrifugal microfluidic platform, Biosens. Bioelectron. 68 (2015) 382–389. https://doi.org/10.1016/j.bios.2014.12.049 LK.

[11] B. Zhu, T. Eurell, R. Gunawan, D. Leckband, Chain-length dependence of the protein and cell resistance of oligo (ethylene glycol)-terminated self-assembled monolayers on gold, J Biomed Mater Res. 56 (2001) 406–416. https://doi.org/10.1002/1097-4636(20010905)56:3<406::aid-jbm1110>3.0.co;2-r.

[12] C.M. Xing, F.N. Meng, M. Quan, K. Ding, Y. Dang, Y.K. Gong, Quantitative fabrication, performance optimization and comparison of PEG and zwitterionic polymer antifouling coatings, Acta Biomater. 59 (2017) 129–138. https://doi.org/10.1016/j.actbio.2017.06.034.

[13] M. Cui, Y. Wang, M. Jiao, S. Jayachandran, Y. Wu, X. Fan, X. Luo, Mixed self-assembled aptamer and newly designed zwitterionic peptide as antifouling biosensing interface for electrochemical detection of alpha-fetoprotein, ACS Sensors. 2 (2017) 490–494. https://doi.org/10.1021/acssensors.7b00103.

[14] A. de los Santos Pereira, S. Sheikh, C. Blaszykowski, O. Pop-Georgievski, K. Fedorov, M. Thompson, C. Rodriguez-Emmenegger, Antifouling polymer brushes displaying antithrombogenic surface properties, Biomacromolecules. 17 (2016) 1179–1185. https://doi.org/10.1021/acs.biomac.6b00019.

[15] J. Benesch, S. Svedhem, S.C.T. Svensson, R. Valiokas, B. Liedberg, P. Tengvall, Protein adsorption to oligo(ethylene glycol) self-assembled monolayers: experiments with fibrinogen, heparinized plasma, and serum, J. Biomater. Sci. Polym. Ed. 12 (2001) 581–597. https://doi.org/10.1163/156856201316883421.

[16] C. Rodriguez-Emmenegger, E. Brynda, T. Riedel, Z. Sedlakova, M. Houska, A.B. Alles,

Interaction of blood plasma with antifouling surfaces, Langmuir. 25 (2009) 6328–6333. https://doi.org/10.1021/la900083s.

[17] O. Pop-Georgievski, Š. Popelka, M. Houska, D. Chvostová, V. Proks, F. Rypáček, Poly(ethylene oxide) layers grafted to dopamine-melanin anchoring layer: Stability and resistance to protein adsorption, Biomacromolecules. 12 (2011) 3232–3242. https://doi.org/10.1021/bm2007086.

[18] G. Wang, X. Su, Q. Xu, G. Xu, J. Lin, X. Luo, Antifouling aptasensor for the detection of adenosine triphosphate in biological media based on mixed self-assembled aptamer and zwitterionic peptide, Biosens. Bioelectron. 101 (2018) 129–134. https://doi.org/10.1016/j.bios.2017.10.024.

[19] Z. Zhang, T. Chao, S. Chen, S. Jiang, Superlow fouling sulfobetaine and carboxybetaine polymers on glass slides, Langmuir. 22 (2006) 10072–10077. https://doi.org/10.1021/la062175d.

[20] W. Yang, H. Xue, W. Li, J.Z. And, S. Jiang, Pursuing "zero" protein adsorption of poly(carboxybetaine) from undiluted blood serum and plasma, Langmuir. 25 (2009) 11911–11916. https://doi.org/10.1021/la9015788.

[21] C. Rodriguez-Emmenegger, B.V.K.J. Schmidt, Z. Sedlakova, V. Šubr, A.B. Alles, E. Brynda, C. Barner-Kowollik, Low temperature aqueous living/controlled (RAFT) polymerization of carboxybetaine methacrylamide up to high molecular weights, Macromol. Rapid Commun. 32 (2011) 958–965. https://doi.org/10.1002/marc.201100176.

[22] C. Zhao, L. Li, J. Zheng, Achieving highly effective nonfouling performance for surface-grafted poly(HPMA) via atom-transfer radical polymerization, Langmuir. 26 (2010) 17375–17382. https://doi.org/10.1021/la103382j.

[23] H. Vaisocherová, V. Ševců, P. Adam, B. Špačková, K. Hegnerová, A. de los Santos Pereira, C. Rodriguez-Emmenegger, T. Riedel, M. Houska, E. Brynda, J. Homola, Functionalized ultra-low fouling carboxy- and hydroxy-functional surface platforms: functionalization capacity, biorecognition capability and resistance to fouling from undiluted biological media, Biosens. Bioelectron. 51 (2014) 150–157. https://doi.org/10.1016/j.bios.2013.07.015.

[24] T. Riedel, F. Surman, S. Hageneder, O. Pop-Georgievski, C. Noehammer, M. Hofner, E. Brynda, C. Rodriguez-Emmenegger, J. Dostálek, Hepatitis B plasmonic biosensor for the analysis of clinical serum samples, Biosens. Bioelectron. 85 (2016) 272–279. https://doi.org/10.1016/j.bios.2016.05.014.

[25] T. Riedel, S. Hageneder, F. Surman, O. Pop-Georgievski, C. Noehammer, M. Hofner, E. Brynda, C. Rodriguez-Emmenegger, J. Dostálek, Plasmonic hepatitis B biosensor for the analysis of clinical saliva, Anal. Chem. 89 (2017) 2972–2977.

https://doi.org/10.1021/acs.analchem.6b04432.

[26] Z. Riedelová, P. Májek, K. Pečánková, J. Kučerová, F. Surman, A. de los Santos Pereira, T. Riedel, SPR biosensor for quantification of fetuin-A as a promising multibiomarker, 67 (2018) 367–375. https://doi.org/10.33549/physiolres.933982.

[27] D. Kotlarek, M. Vorobii, W. Ogieglo, W. Knoll, C. Rodriguez-Emmenegger, J. Dostalek, Compact grating-coupled biosensor for the analysis of thrombin, ACS Sensors. 4 (2019) 2109–2116. https://doi.org/10.1021/acssensors.9b00827.

[28] S. Song, L. Wang, J. Li, C. Fan, J. Zhao, Aptamer-based biosensors, Trends Anal. Chem. 27 (2008) 108–117. https://doi.org/10.1016/j.trac.2007.12.004.

[29] K.M. You, S.H. Lee, A. Im, S.B. Lee, Aptamers as functional nucleic acids: in vitro selection and biotechnological applications, Biotechnol. Bioprocess Eng. 8 (2003) 64–75. https://doi.org/10.1007/BF02940259.

[30] D.M. Jones, A.A. Brown, W.T.S. Huck, P. Street, C. Cb, Surface-initiated polymerizations in aqueous media: effect of initiator density, Langmuir. 18 (2002) 1265–1269. https://doi.org/10.1021/la011365f.

[31] K. Ulbrich, V. Šubr, J. Strohalm, D. Plocová, M. Jelínková, B. Říhová, Polymeric drugs based on conjugates of synthetic and natural macromolecules, J. Control. Release. 64 (2000) 63–79. https://doi.org/10.1016/S0168-3659(99)00141-8.

[32] W. Knoll, M. Liley, D. Piscevic, J. Spinke, M.J. Tarlov, Supramolecular architectures for the functionalization of solid surfaces, Adv. Biophys. 34 (1997) 231–251. https://doi.org/10.1016/S0065-227X(97)89642-6.

[33] C. Stenberg, E., Persson, B., Roos, H., & Urbaniczky, Quantitative determination of surface concentration of protein with surface plasmon resonance using radiolabeled proteins, J. Colloid Interface Sci. 143 (1991) 513–526. https://doi.org/doi.org/10.1016/0021-9797(91)90284-F.

[34] J. Vidic, M. Pla-Roca, J. Grosclaude, M.A. Persuy, R. Monnerie, D. Caballero, A. Errachid, Y. Hou, N. Jaffrezic-Renault, R. Salesse, E. Pajot-Augy, J. Samitier, Gold surface functionalization and patterning for specific immobilization of olfactory receptors carried by nanosomes, Anal. Chem. 79 (2007) 3280–3290. https://doi.org/10.1021/ac061774m.

[35] I. Mihai, A. Vezeanu, C. Polonschii, C. Albu, G.L. Radu, A. Vasilescu, Label-free detection of lysozyme in wines using an aptamer based biosensor and SPR detection, Sensors Actuators, B Chem. 206 (2015) 198–204. https://doi.org/10.1016/j.snb.2014.09.050.

[36] A. Trapaidze, J.P. Hérault, J.M. Herbert, A. Bancaud, A.M. Gué, Investigation of the selectivity of thrombin-binding aptamers for thrombin titration in murine plasma, Biosens. Bioelectron. 78 (2016) 58–66. https://doi.org/10.1016/j.bios.2015.11.017.

[37] P.H. Lin, R.H. Chen, C.H. Lee, Y. Chang, C.S. Chen, W.Y. Chen, Studies of the binding

mechanism between aptamers and thrombin by circular dichroism, surface plasmon resonance and isothermal titration calorimetry, Colloids Surf., B. 88 (2011) 552–558. https://doi.org/10.1016/j.colsurfb.2011.07.032.

[38] J. Müller, D. Freitag, G. Mayer, B. Pötzsch, Anticoagulant characteristics of HD1-22, a bivalent aptamer that specifically inhibits thrombin and prothrombinase, J. Thromb. Haemost. 6 (2008) 2105–2112. https://doi.org/10.1111/j.1538-7836.2008.03162.x.

[39] S. Butenas, C. Van't Veer, K.G. Mann, "Normal" thrombin generation, Blood. 94 (1999) 2169–2178. https://doi.org/10.1182/blood.V94.7.2169.419k22_2169_2178.

[40] J. Müller, T. Becher, J. Braunstein, P. Berdel, S. Gravius, F. Rohrbach, J. Oldenburg, G. Mayer, B. Pötzsch, Profiling of active thrombin in human blood by supramolecular complexes, Angew. Chemie - Int. Ed. 50 (2011) 6075–6078. https://doi.org/10.1002/anie.201007032.

[41] T. Hianik, V. Ostatná, M. Sonlajtnerova, I. Grman, Influence of ionic strength, pH and aptamer configuration for binding affinity to thrombin, Bioelectrochemistry. 70 (2007) 127–133. https://doi.org/10.1016/j.bioelechem.2006.03.012.

[42] K.G. Mann, S. Butenas, K. Brummel, The dynamics of thrombin formation, Arterioscler. Thromb. Vasc. Biol. 23 (2003) 17–25. https://doi.org/10.1161/01.ATV.0000046238.23903.FC.

[43] M. Piliarik, J. Homola, Surface plasmon resonance (SPR) sensors: approaching their limits?, Opt. Express. 17 (2009) 16505. https://doi.org/10.1364/OE.17.016505.

Biographies

Daria Kotlarek graduated with her Masters's degree in Biotechnology at Warsaw University of Life Sciences (Poland) in 2014. Then, she joined Marie Skłodowska-Curie Innovative Training Network BIOGEL as a Ph.D. candidate at the Austrian Institute of Technology and the University of Natural Resources and Life Sciences in Vienna. Her scientific interests embrace biointerfaces, detection and interaction studies of molecular species and surface plasmon resonance-based technologies for application in medical diagnostics and pharma.

Federica Curti graduated with her Master's degree in Biomolecular Chemistry at Parma University (Italy) in 2018. Then, she started her Ph.D. in Chemical Science at the University of Parma in collaboration with the Austrian Institute of Technology in Vienna. Her research interests embrace the synthesis of artificial molecules for sensoristic applications in quality control and medical diagnostic.

Mariia Vorobii graduated with her Master's degree in Pharmaceutical Biotechnology at Lviv Polytechnic National University (Ukraine) in 2014. During 2014-2015, she participate in UNESCO/IUPAC Postgraduate Course in Polymer Science at Institute of Macromolecular Chemistry, Czech Academy of Science. Then, she started her Ph.D. at DWI – Leibniz Institute for Interactive Materials in Aachen under mentorship of Dr. Rodriguez-Emmenegger. Her research interests are surface-initiated controlled radical polymerizations, coating for biomedical devices and membranes with hemocompatibility and antimicrobial properties as well as optical biosensors.

Roberto Corradini obtained his Ph.D. in Chemical Science at University of Parma, 1992 and currently he holds there a professor position. His research interests are in the field of molecular recognition of biologically active species by synthetic molecules. In particular in the last years he has focused on the synthesis of modified PNA and their use in diagnostics and as potential anti-gene or anti-miR drugs.

Maria Careri is Full Professor of Analytical Chemistry at Parma University. Her research activity concerns the development and optimization of methods based on hyphenated techniques (in particular gas and liquid chromatography-mass spectrometry) for food safety and quality. Scientific interests have been also devoted to the application of mass spectrometry-based techniques to structural and functional proteomics for the study of protein biomarkers for the diagnosis of diseases, having as its objective the determination multiplexing marker proteins of clinical interest.

Wolfgang Knoll obtained his PhD in biophysics from University of Konstanz, Germany, in 1976. Has been a director at Max Planck Institute for Polymer Research in Mainz, from 1993-2008. From 2008, he holds managing director position of Austrian Institute of Technology and he serves as a professor in the Department of Nanobiotechnology at the University of Natural Resources and Applied Life Sciences (BOKU). His research interests embrace materials sciences.

Cesar Rodriguez-Emmenegger received his PhD from Charles University in Prague, while working in the Institute of Macromolecular Chemistry, Czech Academy of Sciences under the mentorship of Eduard Brynda (2012). Afterwards he was awarded an Alexander von Humboldt postdoctoral fellowship to work on photoinduced click reactions at interfaces at Karlsruhe Institute of Technology.

Currently, he leads a group on “Superselectivity at biointerfaces” at DWI Leibniz Institute for Interactive Materials. His research interests include: interfacial properties of macromolecules with complex topologies, superselective interfaces, adaptive hemocompatible coatings for medical devices as well as the fabrication of synthetic cell capable of performing simple life-like functions.

Jakub Dostalek received his PhD in physics from Charles University in Prague, Czech republic, in 2006. Then he was a postdoc and project leader at Max Plank Institute for Polymer Research in Mainz, Germany, until 2008. Since 2009, he is with Austrian Institute of Technology in Vienna, Austria, where he was appointed a senior researcher at 2015. His research interests are in the combined aspects of nanophotonics and materials research applied in optical biosensors, light management in thin film optical devices, and polymer-based biointerfaces. He develops analytical technologies for rapid and sensitive detection of chemical and biological species relevant to medical diagnostics and food control.